Tetrahedron Letters 60 (2019) 707–712

Contents lists available at ScienceDirect

Tetrahedron Letters

journal homepage: www.elsevier.com/locate/tetlet

Synthesis and properties of novel extended BODIPYs with rigid skeletons

Yuki Kawamata [a], Satoshi Ito [a,*], Masaru Furuya [a], Kai Takahashi [a], Katsuya Namai [a], Saori Hashimoto [a], Makoto Roppongi [b], Toru Oba [a]

[a] Department of Applied Chemistry, Faculty of Engineering, Utsunomiya University, 7-1-2 Yoto, Utsunomiya, Tochigi 321-8585, Japan
[b] Advanced Instrumental Analysis Department, Center for Industry-University Innovation Support, Utsunomiya University, 7-1-2 Yoto, Utsunomiya, Tochigi 321-8585, Japan

ARTICLE INFO

Article history:
Received 6 October 2018
Revised 12 January 2019
Accepted 18 January 2019
Available online 5 February 2019

Keywords:
BODIPY
Fluorescent dyes
Knoevenagel condensation
Suzuki coupling
retro-Diels–Alder reaction

ABSTRACT

Novel extended BODIPYs fused with bicyclo rings were synthesized from bicyclopyrroles by combining Knoevenagel condensation, Suzuki coupling, and *O*-chelation. The absorption maxima of the BODIPYs ranged from the visible to near-infrared region and the compounds showed good solubility in organic solvents. The solubility of the bicycloBODIPY with 2-naphthyl groups at the α-position of the pyrrole units was particularly high. Heating converted distyrylBODIPY with bicyclo[2.2.2]octene to benzoBODIPY with absorption (748.5 nm) and fluorescence (775.0 nm) in the near-infrared region.

Introduction

Boron-dipyrromethene (BODIPY) dyes exhibit excellent properties, such as high photostability, high fluorescence quantum yields, narrow emission bandwidths, and relatively high absorption coefficients [1]. Therefore, these compounds have been used as laser dyes [2], fluorescence switching materials [3], and chemical sensors [4]. The absorption characteristics of BODIPY dyes can be modulated by introducing various substituents [1a]. Although synthetic methods have been reported that allow access to conjugated extended BODIPY dyes, these derivatives tend to be poorly soluble in organic solvents [5]. In general, conjugated BODIPY dyes require bulky substituents, such as mesityl or *tert*-butyl groups, to increase their solubility. However, this type of substituent often distorts the skeleton of the functional molecule due to steric hindrance. We synthesized novel BODIPY fused bicyclic rings from 1-ethoxycarbonyl bicyclopyrroles **1a–c** [6]. BODIPYs fused with bicyclic rings are expected to have good solubility in organic solvents because the fused bicyclic skeletons inhibit intermolecular π-π interactions, similar to normal bulky substituents [7]. Steric hindrance of the bicyclo rings in the lateral direction is small, so the steric effect on the π-conjugated unit could be reduced by introducing substituents, which should tune the absorption wavelength by σ-π hyperconjugation between the BODIPY unit and the condensed bicyclo rings [8]. Therefore, we synthesized BODIPYs with various bicyclic rings from bicyclopyrroles *via* Knoevenagel condensation, Suzuki coupling, *O*-chelation, and the *retro*-Diels–Alder reaction.

Results and discussion

Extended BODIPYs **4–6** were obtained as shown in Scheme 1 [9]. The ethoxycarbonyl group of bicyclopyrroles **1a–c** was reduced by refluxing with excess $LiAlH_4$ in THF for 2 h. Resulting 2-methyl bicyclopyrroles **2a–c** were converted to the corresponding dipyrromethanes with benzaldehyde in the presence of TFA. The crude dipyrromethanes were oxidized with DDQ, and then reacted with boron trifluoride to afford BODIPYs **3a–c**. BODIPYs **3a–c** exhibited good solubility in organic solvents, such dichloromethane and chloroform. The absorption maxima of **3a**, **3b**, and **3c** were determined as 527, 531.5, and 540 nm, respectively (Fig. 1). The absorption shifts of BODIPYs **3** were ascribed to the differences in the fused-ring skeletons, and were influenced by the σ–π hyperconjugation *via* the bicyclo[2.2.2]octane units. BODIPY **3c** showed the longest wavelength shift because the phenyl group at the crosslinking site showed electron withdrawing properties. This explanation was also supported by the first oxidation potential of BODIPY **3c** being higher than that of BODIPY **3b**.

Next, Knoevenagel condensation of **3a–c** was performed [6]. The Knoevenagel condensation reaction between **3a** and benzaldehyde in a mixture of benzene, acetic acid, and piperidine afforded distyrylBODIPY **4a** in 50% yield alongside a trace amount of monos-

* Corresponding author.
E-mail address: s-ito@cc.utsunomiya-u.ac.jp (S. Ito).

https://doi.org/10.1016/j.tetlet.2019.01.046
0040-4039/

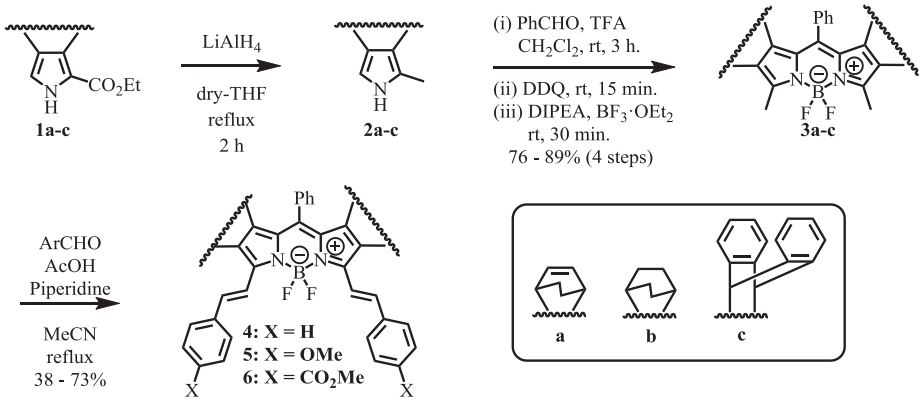

Scheme 1. Synthesis of extended BODIPYs **4**–**6**.

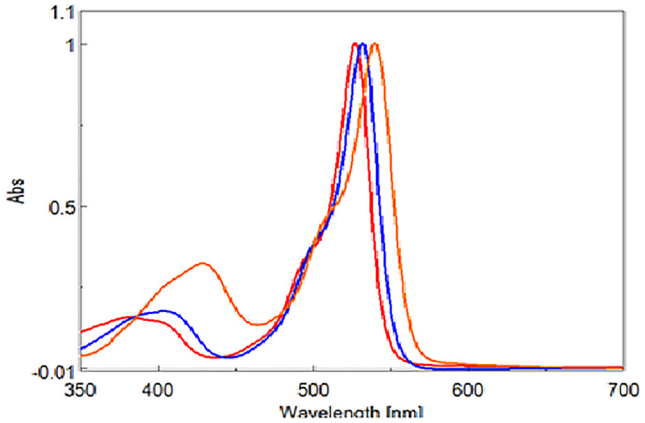

Fig. 1. UV–vis absorption spectra of BODIPYs **3a** (red), **3b** (blue), and **3c** (orange) in $CHCl_3$. (For interpretation of the references to colour in this figure legend, the reader is referred to the web version of this article.)

tyrylBODIPY. Upon changing the solvent from benzene to acetonitrile, the yield of **4a** was improved considerably (73%). This is because the acidity of the allyl protons was increased by using an aprotic polar solvent. BicycloBODIPYs **3b** and **3c** were condensed with benzaldehyde in acetonitrile under similar conditions to afford distyrylBODIPYs **4b** and **4c**. We also synthesized substituted distyrylBODIPYs **5** and **6** from **3**. The absorption maxima of

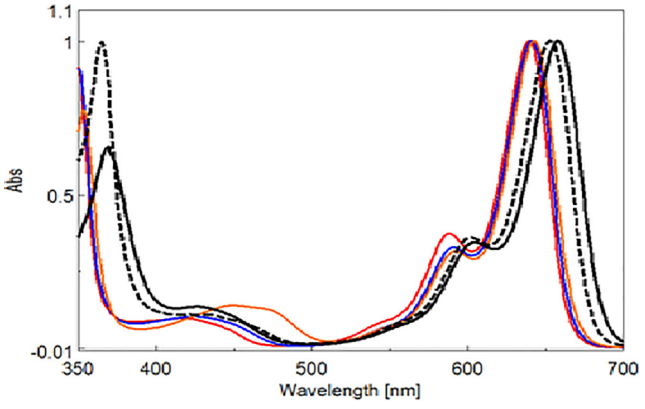

Fig. 2. UV–vis absorption spectra of distyrylBODIPY derivatives **4a** (red), **4b** (blue), **4c** (orange), **5a** (black solid line), and **6a** (black dotted line) in $CHCl_3$. (For interpretation of the references to colour in this figure legend, the reader is referred to the web version of this article.)

4, **5**, and **6** were redshifted by the introduction of the styryl groups compared with the precursors **3** (Fig. 2). DistyrylBODIPY **6a**, synthesized *via* the reaction of **3a** with methyl 4-formylbenzoate and 4-nitrobenzoate, was obtained in a low yield compared with the other distyryl analogues, and an unexpected black powder was formed. The low yield was attributed to the formation of a charge-transfer complex between BODIPY **3a** and the aldehyde. The black powder was dissolved in chloroform and the UV absorption was measured. The solution had a broad absorption in the visible region specific to the CT complex (Figs. 3 and 4). The ^{1}H NMR spectrum of the black powder contained a broad signal indicating the presence of unpaired electrons. In contrast, for BODIPY **3c**, the CT complex was not formed during the same reaction. The steric hindrance of the benzene ring protruding above and below BODIPY **3c** probably prevented the formation of the CT complex.

BicycloBODIPYs **4a, 5a**, and **6a** were converted to benzoBODIPYs **7a**–**c** by heating at 200 °C for 30 min (Scheme 2), which resulted in a dramatic redshift in the position of the absorption maximum (Fig. 5). The absorption and fluorescence maxima of benzoBODIPYs **7a**–**c** were in the near-infrared region. Introducing a methoxy group (**5a**) or ethoxycarbonyl group (**6a**) to the terminal benzene ring of the styrylBODIPYs resulted in a redshift in the maximum absorption wavelength of about 15 nm compared with unsubstituted styrylBODIPY **4a**. (UV: 731.5, 745.5, 748.5 nm; FL: 747.0, 761.0, 775.0 nm).

BODIPYs **11a**–**c** were synthesized using Suzuki coupling to introduce the aryl group at the α-position of the pyrrole (Scheme 3**)**. First, 2-bromobicyclopyrrole **8** was prepared by treating pyrrole **1c** with *N*-bromosuccinimide. 2-Arylpyrroles **9a**–**c** were prepared by Suzuki cross-coupling reactions of 2-bromobicyclopyrrole **8** with arylboronic acids. Removal of the ester groups of pyrroles **9a**–**c** using NaOH afforded compounds **10a**–**c**. Subsequent condensation of **10a**–**c** with benzaldehyde followed by oxidation with DDQ and complexation afforded **11a**–**c**.

The UV–vis absorption spectra of **10a**–**c** are shown in Fig. 6. The absorption maximum of 2-naphthyl derivative **11b** occurred at a longer wavelength than that of 1-naphthyl derivative **11a**. It has

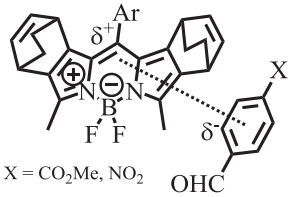

Fig. 3. Formation of a charge-transfer complex between BODIPY derivative **3a** and methyl benzoate with EWG.

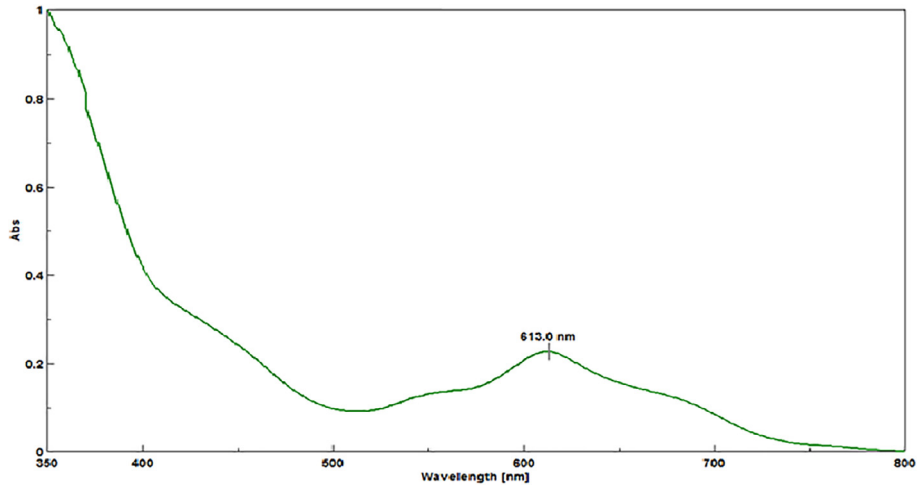

Fig. 4. UV spectrum of CT complex of BIDOPY **3a** and 4-nitrobenzaldehyde in $CHCl_3$.

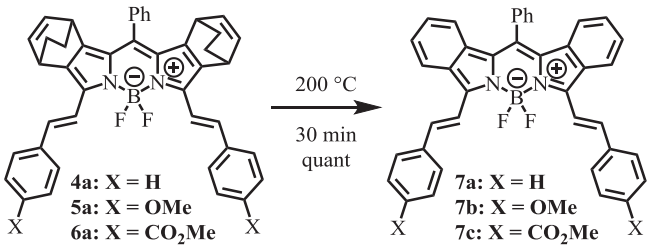

Scheme 2. Synthesis of benzoBODIPYs **7a–c**.

been reported by Schmidt *et al.* that the 2-naphthyl group leads to less steric hindrance than the 1-naphthyl group and can contribute efficiently to conjugated systems [10]. However, the difference in the absorption maximum depending on the substitution position was 35 nm for reported BODIPY derivatives, whereas it was as small as 17 nm for bicycloBODIPY **11b**. This smaller difference is due to the rotation of the naphthyl group being more restricted for BODIPY **11b** as a result of the steric hindrance of the fused-ring skeleton.

The synthesis of *O*-chelate BODIPY **13** was carried out with reference to a reported method [11], as presented in Scheme 4. A 1.0 M solution of boron tribromide in methylene chloride was added dropwise to **11c** and the resulting mixture was purified by column chromatography to afford *O*-chelate BODIPY **13**. The absorption maximum of **13** was redshifted by 73 nm relative to its precursor, **11c**, which was ascribed to the extended conjugation due to the aromatic ring being fixed on the same plane as the BODIPY skeleton (Fig. 7).

The X-ray crystal structure analysis of **13** is presented in Fig. 8 [12–14]. The O–B–O and N–B–N bond angles were determined as 108.2(1)° and 106.5(1)°, respectively. The bond distances of the two N–B bonds were found to be 1.513(2) and 1.505(3) Å, whereas those of the two O–B bonds were found to be 1.466(2) and 1.484(2) Å. BODIPY derivative **13** and reported bicyclo[2.2.2]octane BODIPY have similar structures [11]. These results demonstrated that the fused skeleton has little influence on the structure of the BODIPY skeleton. In contrast, the maximum absorption wavelength of BODIPY **13** was redshifted by 13 nm compared with the previously reported BODIPY [11] due to the σ-π hyperconjugation with the condensed benzene ring through the bicyclo rings.

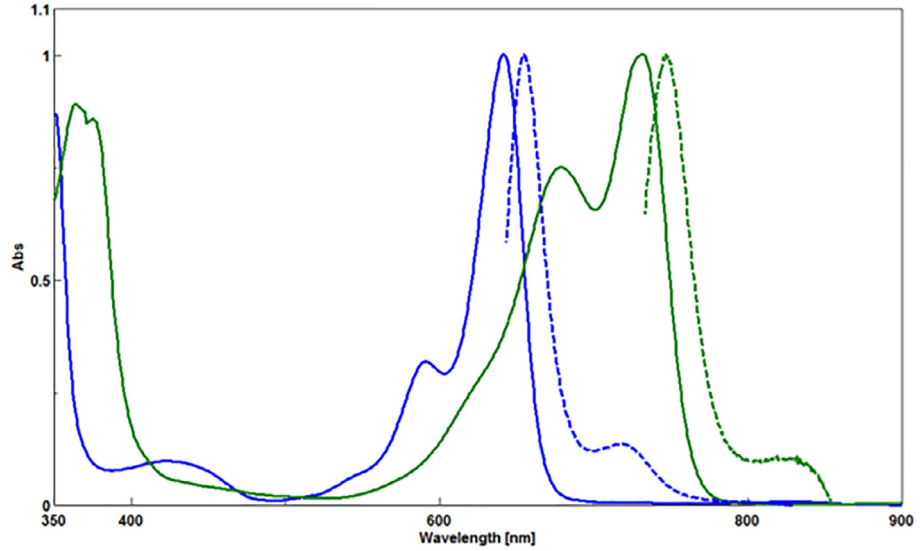

Fig. 5. Absorption (solid line) and emission (dotted line) spectra of BODIPYs **4a** (blue) and **7a** (green) in $CHCl_3$. (For interpretation of the references to colour in this figure legend, the reader is referred to the web version of this article.)

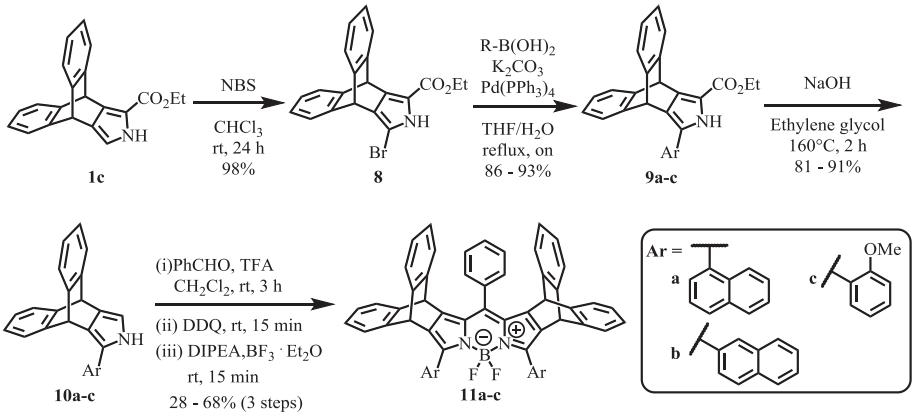

Scheme 3. Synthesis of BODIPYs **11a–c**.

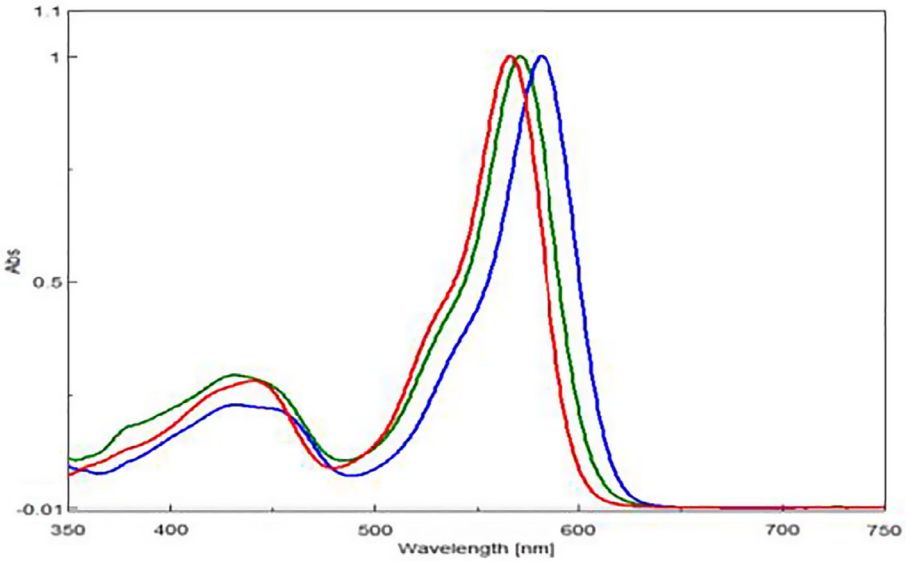

Fig. 6. UV–vis absorption spectra of BODIPYs **11a** (green), **11b** (blue), and **11c** (red) in $CHCl_3$. (For interpretation of the references to colour in this figure legend, the reader is referred to the web version of this article.)

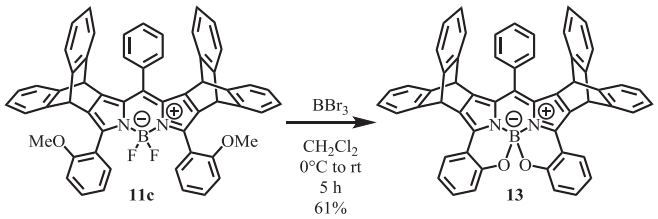

Scheme 4. Synthesis of *O*-chelate BODIPY **13**.

The fluorescence quantum yields (ϕ) of the BODIPYs were not high for this kind of compound, probably because of π-π stacking between molecules or self-quenching due to intramolecular energy transfer. However, the fluorescence lifetimes (τ) of the extended BODIPYs were about 6 ns, which is typical for BODIPYs. *O*-Chelate BODIPY **13** had a longer life span than previously reported analogs, which may be due to the steric hindrance of the benzene rings protruding above and below the plane preventing the intermolecular interaction of the dye moiety [12]. The fluorescence life-time of BODIPY **7a-c** was very short (<4 ns), but two systems determining the fluorescence lifetimes were observed.

Because distyrylbenzoBODIPYs **7a,b** and 2-naphthylBODIPY **11b** have conjugated extended structures, a second oxidation potential was observed for these compounds. The oxidation potential of 2-naphthylBODIPY **11b** was much lower than that of 1-naphthylBODIPY **11a**, suggesting that the π-conjugation expanded in 2-naphthylBODIPY **11b**, which is consistent with the UV measurements. The synthesized BODIPYs showed good solubilities in organic solvent. The solubility of 2-naphthylBODIPY **11b** was particularly high, and was about 10 times that of 1-naphthylBODIPY **11a**. However, the solubility of other extended ring BODIPYs **12a–c** (Fig. 9) was greatly reduced by the introduction of 2-naphthyl groups because of increased intermolecular π-π stacking. Although benzoBODIPY **7a** was expected have lower solubility owing to π-π stacking, it showed good solubility in chloroform (Table 1).

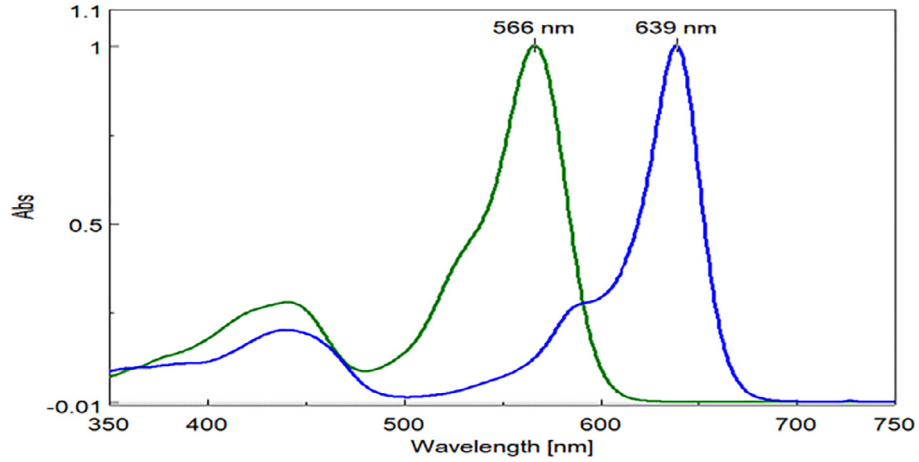

Fig. 7. UV–vis absorption spectra of BODIPYs **11c** (green) and **13** (blue) in $CHCl_3$. (For interpretation of the references to colour in this figure legend, the reader is referred to the web version of this article.)

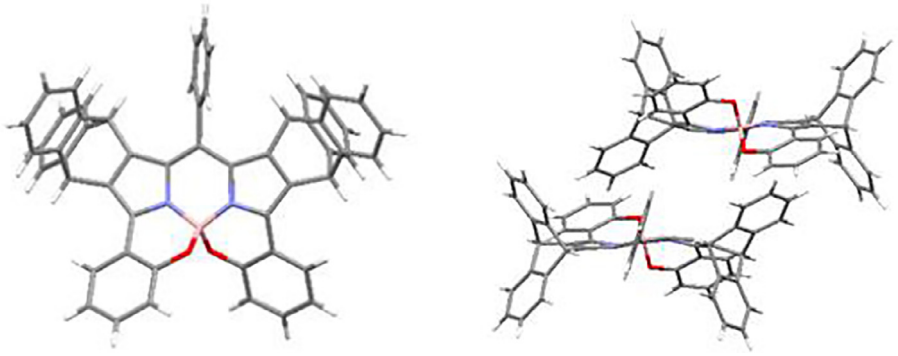

Fig. 8. Crystal structure of *O*-chelate BODIPY **13**.

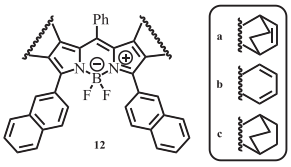

Fig. 9. 2-NaphthylBODIPYs **12a–c**.

Conclusion

We have successfully synthesized novel extended BODIPYs with good solubility using Knoevenagel condensation, Suzuki coupling, and *O*-chelation. By combining the introduction of a fused-ring skeleton into BODIPY and the extension of the conjugation, fine control of the absorption wavelength was possible while maintaining the solubility of the compounds. 2-NaphthylBODIPY **11b** was

Table 1
Physical properties of extended BODIPYs.

	λ_{abs}/nm (log ε)[a]	λ_{em}/nm (Φ)[b]	τ/ns[c]	Solubility in $CHCl_3$ (mg/mL)	E_1^{ox}/V[d]	E_2^{ox}/V[d]	E^{red}/V[d]	E_1^{ox}-E_1^{red}
3a	531.0 (4.75)	546.5 (0.98)	5.95	128	0.63	–	−1.83	2.47
3b	527.0 (4.81)	540.0 (0.51)	5.78	216	0.59	–	−1.96	2.55
3c	540.0 (4.69)	556.5 (0.38)	5.31	292	0.46	–	−1.62	2.08
4a	641.5 (4.99)	654.5 (0.54)	5.58	18	0.42	–	−1.57	1.99
4b	639.5 (4.94)	653.0 (0.55)	5.88	41	0.39	–	−1.47	1.86
4c	643.0 (4.97)	657.5 (0.56)	6.29	68	0.56	–	−1.26	1.82
5a	658.0 (5.09)	677.0 (0.5)	5.52	78	0.28	–	−1.56	1.84
5b	655.5 (5.02)	673.0 (0.54)	5.53	57	0.25	–	−1.62	1.87
5c	662.5 (4.98)	681.0 (0.51)	5.46	40	0.41	–	−1.41	1.82
6a	653.0 (5.03)	667.0 (0.51)	5.60	70	0.54	–	−1.41	1.95
6b	652.0 (5.08)	668.0 (0.52)	5.84	110	0.52	–	−1.43	1.95
6c	651.0 (5.03)	665.0 (0.58)	6.68	98	0.68	–	−1.25	1.93
7a	731.5 (5.05)	747.0 (0.12)	<4	24	0.21	0.34	−1.42	1.63
7b	745.5 (5.10)	761.0 (0.07)	<4	5	0.04	0.49	−1.49	1.53
7c	748.5 (5.09)	775.0 (0.10)	<4	6	0.31	–	−1.28	1.59

(*continued on next page*)

Table 1 (*continued*)

	λ_{abs}/nm (log ε)[a]	λ_{em}/nm (Φ)[b]	τ/ns[c]	Solubility in $CHCl_3$ (mg/mL)	E_1^{ox}/V[d]	E_2^{ox}/V[d]	E^{red}/V[d]	E_1^{ox}-E_1^{red}
11a	571.5 (4.67)	603.5 (0.58)	5.72	22	0.85	–	−1.30	2.15
11b	581.5 (4.74)	612.0 (0.61)	5.99	290	0.42	0.81	−1.44	1.86
11c	566.5 (4.77)	594.0 (0.55)	5.40	21	0.77	–	−1.55	2.32
12a	574.5 (4.85)	605.0 (0.64)	5.39	5	0.65	–	−1.65	2.30
12b	646.0 (5.04)	678.0 (0.67)	6.86	14	0.36	–	−1.46	1.82
12c	570.5 (4.95)	600.0 (0.68)	5.71	11	0.61	–	−1.66	2.27
13	639.0 (4.71)	654.5 (0.49)	10.18	36	0.59	–	−1.50	2.09

[a] In $CHCl_3$.
[b] In CH_2Cl_2 at 10^{-6} M.
[c] Excited at 575 nm in CH_2Cl_2.
[d] *vs*, Ag/$AgNO_3$ in CH_2Cl_2 (Fc = 0 V).

about 10 times more soluble in chloroform than the other derivatives. This synthetic approach represents a powerful tool for developing new functional organic dyes.

Acknowledgments

This work was partially supported by the Cooperative Research Program of 'Network Joint Research Center for Materials and Devices' (No. 20181189), and JSPS KAKENHI Grant Number JP16K05892. We would also like to thank, Mr. Tomokichi Onoda (Shimamura Tech. Co.: Preparative HPLC Systems), Mr. Shota Nakamura (Nihon Waters K. K.: HRMS measuremen), and Mr. Motoya Suzuki (Tokyo Institute of Technology: Fluorescence lifetime measurement).

Appendix A. Supplementary data

Supplementary data to this article can be found online at https://doi.org/10.1016/j.tetlet.2019.01.046.

References

[1] (a) A. Loudet, K. Burgess, Chem Rev. 107 (2007) 4891–4932;
(b) G. Ulrich, R. Ziessel, A. Harriman, Angew. Chem. Int. Ed. 47 (2008) 1184–1201;
(c) R. Ziessel, G. Ulrich, A. Harriman, New J. Chem. 31 (2007) 496–501;
(d) M. Benstead, G.H. Mehl, R.W. Boyle, Tetrahedron 67 (2011) 3573–3601.
[2] (a) L. Marta, B.P. Jorge, P.S. Mercedes, L.A. Fernando, G.M. Inmaculada, C. Angel, I. Lourdes, Sastre Roberto, A.G. Francisco, Org. Lett. 9 (2007) 4183–4186;
(b) K. Gugu, S. Kayode, M. John, N. Tebello, Spectrochim. Acta Part A Mol. Biomol. Spectrosc. 191 (2018) 357–364;
(c) Y. Liutao, L. Ying, M. Chunping, L. Wei, L. Lixin, Dyes Pigm. 122 (2015) 1–5.
[3] (a) T.A. Golovkova, D.V. Kozlov, D.C. Neckers, J. Org. Chem. 70 (2005) 5545–5549;
(b) D. Ciaran, B. Aisling, L. Conor, C. Krzysztof, K. Agnieszka, B. Malgorzata, E.K. Tia, RSC Adv. 7 (2017) 43743–43754;
(c) M. Javier, S. Felix, W. Josef, H. Stefan, Chem. Eur. J. 22 (2016) 1070–1075.
[4] (a) K. Rurack, M. Kollmannsberger, J. Daub, Angew Chem., Int. Ed. 40 (2001) 385–387;
(b) M. Apurba, S. Amit, N. Subhra, K.P. Sanjib, Sens. Actuators, B 255 (2018) 299–308;
(c) J. Yiru, P. Yi, W. Haiying, C. Rong, W. Hua, C. Xinjian, Mater. Chem. Phys. 196 (2017) 262–269.
[5] (a) D. Zeynep, A. Serdar, U. Engin, Akkaya. Tetrahedron 62 (2006) 8484–8488;
(b) J. Chen, A. Burghart, A. Derecskei-Kovacs, K. Burgess, J. Org. Chem. 65 (2000) 2900–2906.
[6] (a) S. Ito, T. Murashima, N.J. Ono, Chem. Soc., Perkin Trans. 1 (1997) 3161–3165;
(b) H. Uno, S. Ito, M. Wada, J. Chem. Soc., Perkin Trans. 1 (2000) 4347–4355.
[7] G. Ulrich, R. Ziessel, A. Harriman, Angew. Chem. Int. Ed. 47 (2008) 1184–1201.
[8] A. Wakamiya, D. Yamazaki, T. Nishinaga, T. Kitagawa, K. Komatsu, J. Org. Chem. 68 (2003) 8305–8314.
[9] (a) M. Wada, S. Ito, H. Uno, T. Murashima, N. Ono, T. Urano, Y. Urano, Tetrahedron Lett. 42 (2001) 6711–6713;
(b) Z. Shen, H. Rohr, K. Rurack, H. Uno, M. Spieles, S. Burkhard, G. Reck, N. Ono, Chem. Eur. J. 10 (2004) 4853–4871.
[10] Y.U. Schmidt, V.N. Zorina, Y.M. Dvorko, I.N. Protsuk, V.K. Belyaeva, G. Clavier, R. Meallet-Renault, T.T. Vu, I.A. Mikhaleva, A.B. Trofimov, Chem. Eur. J. 17 (2011) 3069–3073.
[11] Y. Tomimori, T. Okujima, T. Yano, S. Mori, N. Ono, H. Yamada, H. Uno, Tetrahedron 67 (2011) 3187–3193.
[12] All measurements were made on a Bruker SMART-APEX II CCD plate detector with graphite monochromated Mo-Kα radiation. The data were collected at −173 °C and processed using the APEX II programs from Bruker.
[13] Shelx-2013: Program for the refinement of crystal structures from diffraction data, University of Göttingen, Göttingen, Germany; "Crystal structure refinement with SHELXL". M. G. Sheldrick, Acta Cryst., 2015, C71, 3–15, DOI: org/10.1107/S2053229614024218.
[14] CCDC 1810986 (**13**) contains the crystallographic data for this paper. These data can be obtained free of charge from The Cambridge Crystallographic Data Centre via www.ccdc.cam.ac.uk/data_request/cif.